Journal of Statistical Theory and Practice (2023) 17:46
https://doi.org/10.1007/s42519-023-00343-6

ORIGINAL ARTICLE

Stochastic Simulation of Continuous Time Random Walks: Minimizing Error in Time-Dependent Rate Coefficients for Diffusion-Limited Reactions

Matthew A. Grayson[1,2] · **Alain Kangabire**[1] · **Can Aygen**[1] · **Kevin Considine**[1]

Accepted: 13 August 2023 / Published online: 5 September 2023
© Grace Scientific Publishing 2023

Abstract

A reaction limited by standard diffusion is simulated stochastically to illustrate how the continuous time random walk (CTRW) formalism can be implemented with minimum statistical error. A step-by-step simulation of the diffusive random walk in one dimension reveals the fraction of surviving reactants $P(t)$ as a function of time, and the time-dependent unimolecular reaction rate coefficient $K(t)$. Accuracy is confirmed by comparing the time-dependent simulation to results from the analytical master equation, and the asymptotic solution to that of Fickian diffusion. An early transient feature is shown to arise from higher spatial harmonics in the Fourier distribution of walkers between reaction sites. Statistical 'shot' noise in the simulation is quantified along with the offset error due to the discrete time derivative, and an optimal simulation time interval Δt_0 is derived to achieve minimal error in the finite time-difference estimation of the reaction rate. The number of walkers necessary to achieve a given error tolerance is derived, and $W = 10^7$ walkers is shown to achieve an accuracy of $\pm 0.2\%$ when the survival probability reaches $P(t) \sim \frac{1}{3}$. The stochastic method presented here serves as an intuitive basis for understanding the CTRW formalism, and can be generalized to model anomalous diffusion-limited reactions to prespecified precision in regimes where the governing wait-time distributions have no analytical solution.

✉ Matthew A. Grayson
m-grayson@northwestern.edu

Alain Kangabire
alainkangabire2022@u.northwestern.edu

Can Aygen
canaygen@u.northwestern.edu

Kevin Considine
kevinconsidine2024@u.northwestern.edu

1 Electrical and Computer Engineering, Northwestern University, 2145 Sheridan Rd, Evanston, IL 60208, USA

2 Program in Applied Physics, Northwestern University, 2145 Sheridan Rd, Evanston, IL 60201, USA

Keywords Diffusion limited reaction · Diffusion controlled reaction · Random walk · Transients · Noise analysis · CTRW

1 Introduction

Relaxation dynamics of disordered systems can often be modeled as a reaction process limited by diffusion. If the diffusion is standard and obeys Fick's law, then the diffusion coefficient is a constant, and the reactant concentration will decay exponentially at long times. Such reactions are quite common and include (pseudo)unimolecular chemical reactions in solution at room temperature. On the other hand, diffusion in more strongly disordered systems can be governed by a diffusion coefficient with explicit time-dependence, frequently containing a power-law in time. When such diffusion is the limiting step of a reaction, the reactant concentration decays more slowly than an exponential at long times. One example of this is the stretched exponential Kohlrausch-Williams-Watts relaxation. These slow relaxations have been observed in a wide range of fields including conductivity in amorphous solids [1], photocurrent in organic and inorganic materials [2], and dielectric relaxation in polymers [3] among others, and can apply to both unimolecular and bimolecular reactions [4]. A microscopic model that can describe the dynamics of both standard and anomalous diffusion is the continuous-time random walk theory (CTRW) [5], whereby each step of the diffusive random walk is governed by a wait-time distribution function $\psi(\tau)$ predicting the probability $\psi(\tau)d\tau$ for the subsequent step to be taken within $d\tau$ of the wait time τ. In spite of the power of the CTRW theory, this formalism has, to date, been solved primarily with analytical expressions and even then, for only a limited number of proposed analytical wait time distribution functions [4, 6–8].

Therefore, this work will stochastically simulate the well-known case of a diffusion-limited reaction limited by standard diffusion in order to validate the stochastic simulation method and quantify its accuracy. CTRW theory was first proposed by Montroll and Weiss [9] as a generalized framework for describing arbitrary diffusion processes. Here we focus on the simplest choice for $\psi(\tau)$, a Poissonian wait time distribution. We then perform stochastic simulations of the CTRW by generating an appropriately distributed sequence of wait times for a statistical ensemble of walkers while querying the walk at regular intervals in measurement time. Using the results from these stochastic studies, we deduce key descriptors of the diffusion in-progress, such as the time-dependent normalized distribution of walkers $p(x, t)$, and, in the presence of a reaction, the time-dependent fraction of surviving walkers $P(t)$ and reaction rate coefficient $K(t)$. Finally, we confirm the accuracy of our simulations by comparing to the analytical solutions of the master equation for standard diffusion, which asymptotically arrives at the Fickian limit. We find good agreement between stochastic simulation and analytical results for the calculated rate coefficients $K(t)$ at the limit of infinitesimal step distance. The stochastic method described here can be adapted to simulate arbitrary reaction kinetics starting from the initial transient response at $t = 0$ to the final asymptotic relaxation. Cases of interest include an inhomogeneous initial distribution of reactants, anomalous diffusion limited reactions [4, 6], and surface reaction kinetics, such as the Langmuirinshelwood and Eleyideal mech-

anisms [10]. The underlying CTRW formalism has proven useful in many fields that describe dynamics in complex systems, such as biophysics [11, 12], and the CTRW model forms the microscopic basis for complex kinetics that can be asymptotically described with fractional calculus [13].

2 Random Walk Formalism

This section will review the original CTRW formalism for the sake of completeness and establish notation specific to this manuscript. For readers unfamiliar with random walk theory, the authors highly recommend the classic introductory review text by Montroll [14], and subsequently the foundational Montroll & Weiss paper which introduced CTRW theory [9], with the key results of CTRW theory summarized succinctly by Shlesinger [1] and discussed in greater depth by Klafter and Sokolov [15].

In CTRW, walkers move in space-time by following the same rules at each step. The rules that describe a single step of a walker therefore determine the dynamics of the entire random walk and are specified through functions $p(\boldsymbol{\xi})$, the probability density function for a relative displacement vector $\boldsymbol{\xi}$ at a given step, and $\psi(\tau)$, the probability density for the wait time τ between successive steps. These probability functions are normalized [16]:

$$\int_{\mathbb{R}^n} p(\boldsymbol{\xi}) d\boldsymbol{\xi} = 1 \tag{1}$$

where n is the dimensionality of the displacement vector and

$$\int_0^\infty \psi(\tau) d\tau = 1. \tag{2}$$

In this work, the space will be simplified to a 1D lattice, and the step displacement ξ discretized to ra, where r is an integer and a the lattice spacing. In this regard, the spatial probability density is replaced by a probability mass function $p(\xi)$ for discrete relative positions ξ, and the normalization integral of Eq. (1) by a discrete sum over these relative lattice positions:

$$\sum_\xi p(\xi) = 1. \tag{3}$$

The probability distribution in step time $\psi(\tau)$, however, remains continuous, hence the name attributed to this theory.

The nth step probability mass function $p_n(x)$ to find the walker at position x after $n \geq 1$ steps recursively satisfies the convolution sum [9]:

$$p_n(x) = \sum_\xi p_{n-1}(x - \xi) p(\xi) \tag{4}$$

where $p_0(x)$ describes the initial spatial probability mass function of the walkers at the start of the random walk. For example, $p_0(x) = \delta(x)$ would represent a Kronecker delta function if the walker starts at the origin. In the absence of any mechanism to annihilate walkers, the total probability is conserved at every step,

$$\sum_x p_n(x) = 1. \tag{5}$$

Analogous to the spatial recursion of Eq. (4), the probability density $\psi_n(t)$ to take the nth step at time t is recursively defined with a convolution integral [9],

$$\psi_n(t) = \int_0^t \psi_{n-1}(t-\tau)\psi(\tau)d\tau \tag{6}$$

Using $p_n(x)$ and $\psi_n(t)$, one can determine the probability mass function $q(x,t)$ that the walker landed at position x exactly between time t and $t+dt$, regardless of how many steps it took to get there [9].

$$q(x,t)dt = \sum_{n=0}^{\infty} p_n(x)\psi_n(t)dt \tag{7}$$

We further define the idling probability $\phi(t)$ *not* to have taken a subsequent step within a time interval t as [9]

$$\phi(t) = 1 - \int_0^t \psi(\tau)d\tau \tag{8}$$

The product of $q(x,t')$ and $\phi(t-t')$ therefore gives the probability that the walker arrived with any integer number of steps at position x some time t' earlier and has remained idle thereafter without taking any subsequent steps. The walker's normalized probability function $p(x,t)$ to be at position x at time t is therefore the convolution over all possible idling times of arriving at that position and subsequently not moving [9]

$$p(x,t) = \int_0^t q(x,t')\phi(t-t')dt' \tag{9}$$

3 Model of Unimolecular Reaction

A simple representation of a diffusion-limited reaction can now be simulated stochastically. The diffusion of the reactant is simulated by the random walk, and the reaction is modeled as a contact interaction with site specific annihilation of the walkers at trap sites $\pm x_{\text{tr}}/2$ representing a trap density $n_{\text{tr}} = 1/x_{\text{tr}}$. In the language of a bimolecular reaction, the minority reactant is represented by the mobile walkers and the majority reactant is represented by stationary traps that annihilate walkers upon contact. Since

the concentration of annihilation sites is unchanged, the reaction is effectively unimolecular. In keeping with the unimolecular nature of the reaction, it is assumed that the traps can annihilate an arbitrary number of walkers, resulting in a minority reactant concentration that vanishes at long times, and a majority reactant concentration that remains unchanged.

The reaction modifies the spatial recursive relation of Eq. (4) and the probability conservation law of Eq. (5) from the standard random walk formalism. The spatial recursive relation will remain valid only in the spatial interval between traps, whereas the traps will force the concentration of walkers at each trap site $\pm x_{\text{tr}}/2$ to zero, acting as nodes in the spatial distribution function:

$$p_n(x) = \begin{cases} \sum_\xi p_{n-1}(x-\xi)p(\xi) & \text{for } |x| < \frac{x_{\text{tr}}}{2} \\ 0 & \text{for } |x| \geq \frac{x_{\text{tr}}}{2} \end{cases} \tag{10}$$

A unitless trap distance $S = x_{\text{tr}}/a$ counts the number of steps of size a between the two traps, where the continuum limit with inifinitesimal step size is reached as $S \to \infty$ for fixed x_{tr}.

Note that under the reactive boundary conditions of Eq. (10), the normalization condition in Eq. (5) is no longer necessarily valid at increasing step index, since as n increases more walkers can reach the reactive trap sites where their contribution to the total probability is annihilated. Summing $p(x,t)$ from Eq. (9) over all positions gives the time dependent fraction of surviving walkers $P(t)$:

$$P(t) = \sum_{x=-x_{\text{tr}}/2}^{+x_{\text{tr}}/2} p(x,t) \tag{11}$$

And from this, the rate coefficient $K(t)$ for a unimolecular reaction is calculated [6]:

$$K(t) = -\frac{1}{P(t)} \times \frac{d}{dt} P(t) = -\frac{d}{dt} \ln P(t), \tag{12}$$

which by inspection would yield a constant rate coefficient K if $P(t)$ were an exponential decay.

To validate the stochastic methods employed here, the reaction coefficient $K(t)$ deduced from three different methods will be compared. First, Sect. 4 details the stochastic description of the diffusion-limited reaction according to CTRW. Second, Sect. 5 uses the master equation to solve for the same. Finally, Sect. 6 compares the well-known asymptotic rate constant for reactions limited by simple Fickian diffusion. In each of the three descriptions, there will be an initial distribution of walkers normalized to the Kronecker delta function at the origin

$$p(x,0) = \delta(x). \tag{13}$$

Unlike prior CTRW analyses which deliberately randomize the starting position of the walker [4, 6, 17–19], here the starting condition $\delta(x)$ represents many equally

weighted Fourier components of the distribution so that this initial response can be quantified. To illustrate the simulation with the simplest symmetric random walk, we choose the characteristic probability function

$$p(\xi) = \begin{cases} 0.5 & \text{for } \xi = a \\ 0.5 & \text{for } \xi = -a \\ 0 & \text{otherwise} \end{cases} \tag{14}$$

and a Poissonian wait time distribution [6, 19]

$$\psi(\tau) = \frac{1}{T} e^{-\tau/T}, \tag{15}$$

where T is the characteristic average wait-time between steps of the walkers.

4 Stochastic Simulation of Diffusion-Limited Unimolecular Reaction

A method for stochastic simulation of a random walk is now demonstrated according to the CTRW formalism. A time-dependent stochastic distribution of surviving walkers $p(x, t)$ normalized to unity at $t = 0$ is generated by simulating an ensemble of W continuous time random walks for times $0 < t \leq t_f$, where t_f is the maximum duration of the simulation. The walkers are indexed $w \in 1, \ldots W$, and according to Eq. (13) each step of the wth walker obeys the spatial $p(\xi)$ and temporal $\psi(\tau)$ distribution functions of Eqs. (14) and (15), respectively, as follows.

To determine the random wait-time interval τ_n between the $(n-1)$th and nth steps that obeys the wait-time distribution function, the inverse transform sampling method is used [20]. The cumulative distribution function up to the wait-time τ will yield a number between 0 and 1,

$$C(\tau) = \int_0^\tau \psi(\tau')d\tau'; \quad 0 \leq C(\tau) < 1. \tag{16}$$

So a set of uniformly distributed random numbers is first created within the interval $y_n \in [0, 1)$. Then the inverse of this set $\tau_n = C^{-1}(y_n)$ will contain random wait times for single steps distributed according to $\psi(\tau)$. For the Poissonian $\psi(\tau)$ specified in Eq. (15), the cumulative distribution is

$$C(\tau) = 1 - e^{-\frac{\tau}{T}} \tag{17}$$

with inverse,

$$C^{-1}(y) = -T \ln(1 - y). \tag{18}$$

A stochastic simulation of the CTRW formalism will now provide the position- and time-dependent probability distribution $p(x, t)$. First, a set of random wait-time

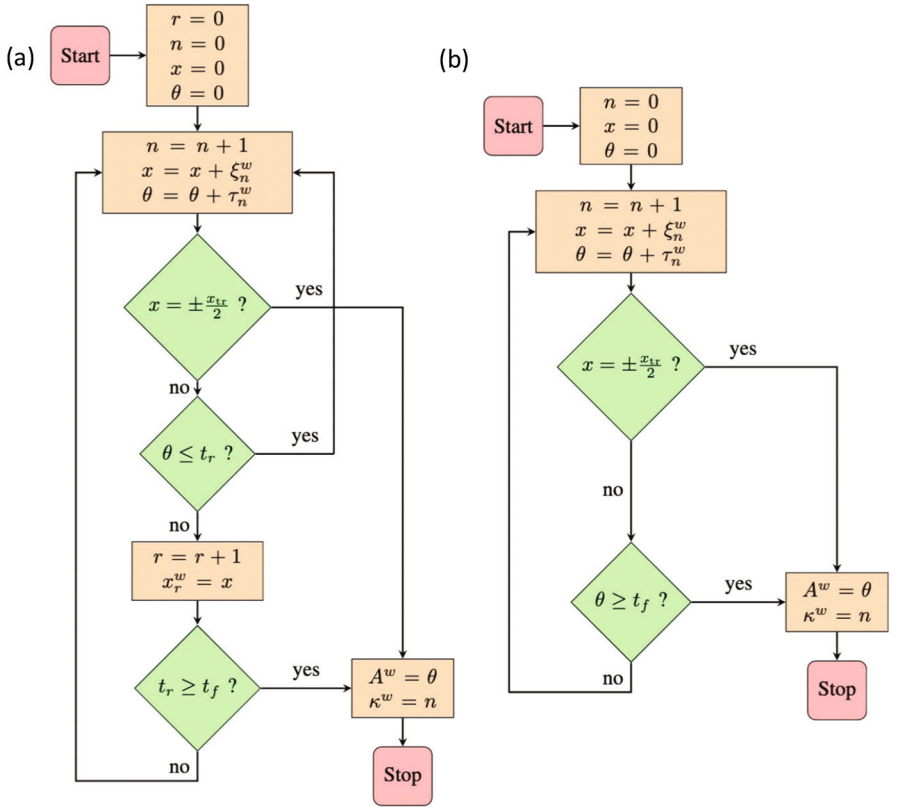

Fig. 1 **a** Stochastic algorithm flow chart for the wth walker to determine the position x_r^w at the rth reporting time, as well as the age of the walker A^w and kill index κ^w when the walker is annihilated by reacting at the trap site $\pm x_{\text{tr}}/2$. **b** If the spatial distribution does not need to be recorded, a simplified algorithm accelerates calculation of the age A^w and kill index κ^w for each walker, *without* tracking the position at reporting times t_r

intervals τ_n^w and random step displacements ξ_n^w is generated for the n steps of the wth walker to obey the probability distributions $\psi(\tau)$ and $p(\xi)$, respectively. Assume a set of R reporting times of interest t_r indexed by $r \in 1, 2, ...R$.

The flow chart of Fig. 1a illustrates how the instantaneous position x_r^w of the wth walker can be determined at reporting times t_r. Let the position of the walker of interest for the nth step be notated with the variable x,

$$x = \sum_{i=0}^{n} \xi_i^w, \tag{19}$$

and let the position at reporting time t_r be recorded as x_r^w. Two asynchronous time scales are tracked, namely the cumulative step time θ after n steps,

$$\theta = \sum_{i=0}^{n} \tau_i^w, \tag{20}$$

and the reporting time t_r. Correspondingly, two asynchronous time increment loops are run in Fig. 1a: one which increments the step index '$n = n + 1$' if the cumulative step time θ is less than the current reporting time, and one which increments the reporting time index '$r = r+1$', otherwise. Both loops have asynchronous termination conditions: the step-increment loop is terminated if the walker lands on a trap $x = \pm x_{\text{tr}}$, and the reporting time increment loop is terminated if the final reporting time is reached. Either termination condition sets the age of the walker $A^w = \theta$ and the kill index $\kappa^w = n$ of how many steps that walker took to reach the trap. Note that the 0th wait time τ_0^w and step displacement ξ_0^w represent the starting time and starting position of the wth walker.

Averaging the ensemble of x_r^w positions for all walkers at a given reporting time t_r yields the distribution $p(x, t_r)$:

$$p(x, t_r) = \frac{1}{W} \sum_{w=1}^{W} \delta(x - x_r^w)\Theta(A^w - t_r) \tag{21}$$

where $\delta(x)$ is the Kronecker delta and $\Theta(x)$ is the Heaviside step function that counts only surviving walkers whose age exceeds the reporting time $A^w \geq t_r$. An example of the statistical ensemble average $p(x, t_r)$ is plotted with dots in Fig. 2, where the distribution at early times before the walkers reach the traps resembles a Gaussian, and the distribution at later times converges to a cosine function with nodes at the traps at $x_{\text{tr}} = \pm 1/2$. The total probability of survival $P(t_r)$ as a function of time can then be deduced from the spatial summation of Eq. (21) per Eq. (11).

If the spatial distribution $p(x, t_r)$ is *not* needed, a faster and more computationally efficient way to directly deduce the survival probability $P(t_r)$ can be used, as illustrated in Fig. 1b. This alternative approach is particularly helpful when only time derivatives of the survival probability need to be estimated, in which case the $r \in (1, 2, \ldots R)$ indexed reporting times will be taken at regular intervals $t_r = r\frac{t_f}{R}$ defined in terms of a total simulated time duration t_f. From the resulting ages A^w, $P(t_r)$ can be computed as follows

$$P(t_r) = \frac{1}{W} \sum_{w=1}^{W} \Theta(A^w - t_r) \tag{22}$$

From either method of determining the stochastic survival probability $P(t_r)$, the reaction rate coefficient $K(t_r)$ can be approximated using a discrete double-sided derivative approximation to the logarithmic derivative in Eq. (12):

$$K(t_r) = -\frac{1}{P(t_r)} \frac{P(t_{r+1}) - P(t_{r-1})}{2\Delta t}. \tag{23}$$

Employing the displacement probability $p(\xi)$ of Eq. (14) and the Poissonian wait time distribution $\psi(\tau)$ of Eq. (15), the resulting fraction of surviving walkers $P(t_r)$ and reaction rate $K(t_r)$ are plotted with dots in Fig. 3 panels (a) and (b), respectively, with panel (c) zooming into the noise around the asymptotic value of $K(t_r)$. In addition, the

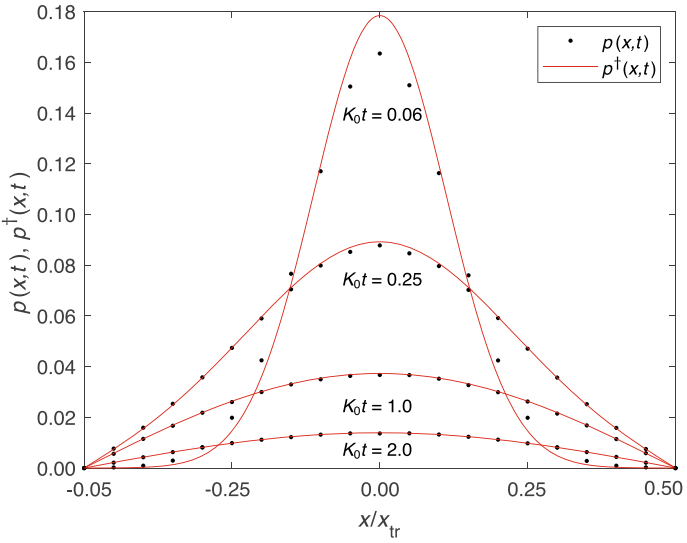

Fig. 2 Stochastic simulations of $p(x, t_l)$ (circles) at different times compared to the analytical solution $p^\dagger(x, t)$ in the spatial continuum limit (lines) for a diffusion-limited unimolecular reaction with diffusion constant $D = 1$, trap position $x_{\rm tr} = 0.5$, number of steps between the origin and traps $S = 20$, giving a lattice spacing $a = 1/20$, wait-time distribution time constant $T = 1/200$, and characteristic reaction rate $K_0 = \pi^2/4$. The number of walkers is $W = 10^6$. The plots of the continuum limit are generated from Eq. (33) where the sum is terminated at $|j| \leq 100$. The times shown represent $K_0t \approx 0.06, 0.25, 1.0$, and 2.0 demonstrating rapid decay of all but the lowest cosine harmonic for $K_0t \gtrsim 1$

statistical average $\langle K(t)\rangle$ over a range of data $r = \{1 \ldots R\}$ such that $J < K_0t_r < J+1$ for integer J is plotted with open circles,

$$\langle K(t)\rangle = \frac{1}{R}\sum_{r=1}^{R} K(t_r), \tag{24}$$

and the standard deviation $\delta K(t)$ over the same range is plotted with error bars,

$$\delta K(t) = \frac{1}{R}\sum_{r=1}^{R}[K(t_r) - \langle K(t)\rangle]^2. \tag{25}$$

5 Master Equation for Diffusion-Limited Unimolecular Reaction

To validate the accuracy of these stochastic simulations, the next section will use a master equation to derive an analytical expression for the same diffusion-limited reaction in the spatial continuum limit. In this limit, the step distance a and the characteristic step wait time T both vanish while the limit value of the corresponding diffusion coefficient D remains constant and finite. The same spatial and temporal variable names

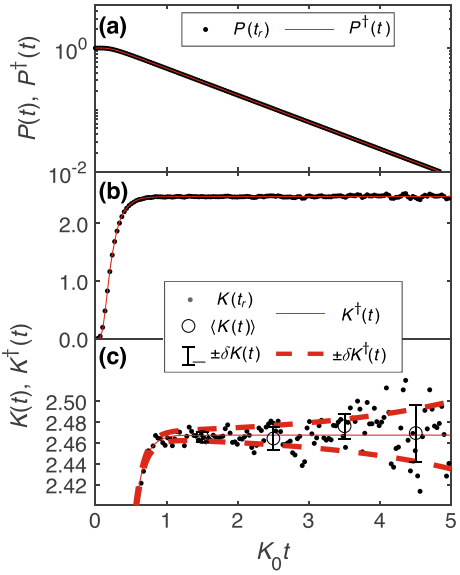

Fig. 3 Comparison between stochastic simulation and analytical solution for a diffusion-limited unimolecular reaction with Poissonian wait-time distribution function $\psi(\tau)$. **a** Stochastic $P(t_r)$ and analytical $P^\dagger(t)$ in log-lin plot versus time. **b** Stochastic $K(t_r)$ and analytical $K^\dagger(t)$ in lin-lin plot versus time. **c** The stochastic $K(t_r)$, average $\langle K(t)\rangle$ and standard deviation $\pm\delta K(t)$ of the local ensemble of statistical values are plotted as dots, open circles, and error bars, respectively. The standard deviation of the noise in the stochastic simulation $\delta K(t)$ matches well with the analytical noise prediction $\delta K^\dagger(t)$ of Eq. (45) (red dashed line). The simulation employs a normalized diffusion constant $D = 1$ and trap position $x_{\rm tr} = \pm 1/2$, with the number of steps between the origin and the traps $S = 40$, giving a lattice spacing $a = 1/40$, wait-time distribution time constant $T = 1/800$, and characteristic reaction rate $K_0 = \pi^2/4$. The number of walkers is $W = 10^7$

will be used as in the previous section, with probabilities and rates superscripted with a dagger to differentiate the analytical solution from the statistically derived case, i.e. $p^\dagger(x,t)$, $P^\dagger(t)$, and $K^\dagger(t)$.

CTRW theory can determine the appropriate infinitesimal step parameters to compare with the stochastic random walk. Montroll [16] showed that any CTRW with a wait time distribution having a first moment and a spatial step distribution having both first and second moments behaves like standard diffusion at long times [9]. The explicit relationship of these moments to the diffusion coefficient [16], is shown below for the spatial and wait-time distributions under consideration from Eqs. (14) and (17):

$$\langle \xi \rangle = \sum_{\xi=-\infty}^{\infty} \xi\, p(\xi) = 0, \tag{26}$$

$$\langle \xi^2 \rangle = \sum_{\xi=-\infty}^{\infty} \xi^2 p(\xi) = a^2, \tag{27}$$

$$\langle \tau \rangle = \int_0^{\infty} \tau \psi(\tau) d\tau = T, \tag{28}$$

from which the diffusion coefficient can be determined, accordingly,

$$D = \frac{\langle \xi^2 \rangle - \langle \xi \rangle^2}{2\langle \tau \rangle} = \frac{a^2}{2T} = \frac{x_{\text{tr}}^2}{2S^2 T}. \tag{29}$$

This relation can be inverted to choose different discrete random walk parameters a and T that all correspond to the same diffusion constant D. For example, as the lattice spacing a between step sites vanishes and the number of steps S increases, the characteristic wait time of the Poisson distribution should vanish as

$$T = \frac{a^2}{2D} = \frac{x_{\text{tr}}^2}{2DS^2}, \tag{30}$$

whereby D remains fixed.

Now that the diffusion coefficient corresponding to the continuum limit has been determined, the analytical solution can be derived for the Fickian diffusion problem between two symmetrically positioned traps. First in the absence of traps, the standard master equation for Fickian diffusion,

$$\frac{\partial G^\dagger(\mathbf{x}, t)}{\partial t} = D\, \nabla^2 G^\dagger(\mathbf{x}, t), \tag{31}$$

has the well-known time-dependent Gaussian solution for the specialized 1D case where all walkers start at the origin

$$G^\dagger(x, t) = \frac{a}{\sqrt{4\pi Dt}} e^{-\frac{x^2}{4Dt}}, \tag{32}$$

where the lattice spacing factor a normalizes the continuous probability density to match the discrete probability per lattice site.

In the presence of a reaction, the analytical solution to the Fickian master equation Eq. (31) must vanish at the reactive traps $x = \pm x_{\text{tr}}/2$. As illustrated in Fig. 4, a linear superposition of periodically translated functions $G(x - jx_{\text{tr}}, t)$ with alternating signs $(-1)^j$ for integers $j \in (\ldots -2, -1, 0, 1, 2, \ldots)$, leads to a solution having nodes at $x = \pm x_{\text{tr}}/2$, while still satisfying homogeneous diffusion between $-x_{\text{tr}}/2 < x < x_{\text{tr}}/2$:

$$p_0^\dagger(x, t) = \sum_{j=-\infty}^{\infty} (-1)^j G\,(x - jx_{\text{tr}}, t) \quad |x| \le x_{\text{tr}}/2 \tag{33}$$

Figure 4 illustrates the positive (blue) and negative (red) contributions of these translated Gaussians for this case, with the solution for $p_0^\dagger(x, t)$ shown in the interval $-x_{\text{tr}}/2 < x < +x_{\text{tr}}/2$ (black).

Using Fourier analysis (derivation in "Appendix"), the explicit spatial dependence in the domain $x < |x_{\text{tr}}/2|$ is observed to consist of odd cosine harmonics with nodes

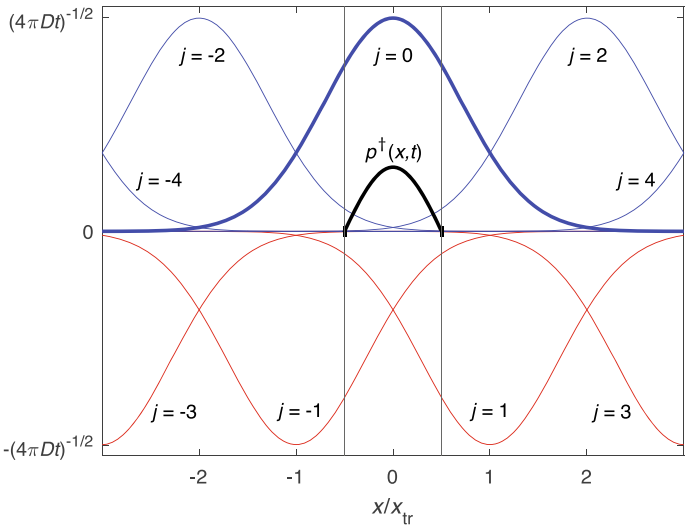

Fig. 4 Fickian master equation in the continuum approximation $p^{\dagger}(x,t)$ of the probability distribution (black curve) for a diffusion-limited reaction with walkers all starting at the origin and reactive trap sites at $x/x_{tr} = \pm 1/2$ indicated by vertical lines. Conceptually, $p^{\dagger}(x,t)$ can also be represented as a linear superposition of the displaced positive (blue) and negative (red) Gaussian solutions to the homogeneous diffusion equation Eq. (31). Such a periodic superposition guarantees nodes at $x = \pm x_{tr}/2$

at $x = \pm x_{tr}/2$ whose higher harmonics $(2\nu + 1)$ decay much faster with time:

$$p^{\dagger}(x,t) = \frac{1}{2x_{tr}} \sum_{\nu=0}^{\infty} \exp\left\{ -\left[\frac{\pi(2\nu+1)}{x_{tr}}\right]^2 Dt \right\} \times \cos\left[(2\nu+1)\frac{\pi}{x_{tr}}x\right]. \tag{34}$$

The decay rate of the fundamental $\nu = 0$ term is $K_0 = D(\pi/x_{tr})^2$, with higher order cosine harmonics vanishing much faster with decay rates $K_\nu = (2\nu+1)^2 K_0$. For example, the $\nu = 1$ decay term is already e^{-8} times smaller than the $\nu = 0$ term when $K_0 t = 1$. Reexamination of Fig. 2 clearly shows how at increasing time intervals the solution rapidly decays to the fundamental cosine distribution.

Spatially integrating over the interval between the traps, the time-dependent fraction of surviving walkers becomes

$$P^{\dagger}(t) = \frac{4}{\pi} \sum_{\nu=0}^{\infty} \frac{(-1)^{\nu}}{2\nu+1} \exp\left\{ -\left[\frac{\pi(2\nu+1)}{x_{tr}}\right]^2 Dt \right\}. \tag{35}$$

In Fig. 3, this analytical solution $P^{\dagger}(t)$ is observed to lie directly on top of the stochastic solution $P(t)$, confirming its validity. The unimolecular reaction coefficient for the infinitesimal step limit $K^{\dagger}(t)$ is defined identically to Eq. (12), and, again, Fig. 3 shows excellent agreement between the analytical $K^{\dagger}(t)$ and the noise averaged value $\langle K(t) \rangle$.

6 Asymptotic Limit for Diffusion-Limited Unimolecular Reaction

The asymptotic limit for the infinitesimal step probability distribution $p^{\dagger}(x,t)$ is dominated by the slowest decaying $\nu = 0$ term in the sum of Eq. (34). The spatial dependence at long times is therefore a simple cosine with nodes at $x = \pm x_{\mathrm{tr}}/2$ and an antinode at $x = 0$:

$$\lim_{t\gg 0} p^{\dagger}(x,t) = \frac{1}{2x_{\mathrm{tr}}} \exp\left[-\left(\frac{\pi}{x_{\mathrm{tr}}}\right)^2 Dt\right] \cos\left(\frac{\pi}{x_{\mathrm{tr}}}x\right) \tag{36}$$

The spatial integral of this yields a simple exponential decay for the time dependent fraction of surviving walkers:

$$\lim_{t\gg 0} P^{\dagger}(t) = \frac{4}{\pi} \exp\left[-\left(\frac{\pi}{x_{\mathrm{tr}}}\right)^2 Dt\right] \tag{37}$$

Substituting this asymptotic behavior into Eq. (12), gives the expected time-independent unimolecular rate coefficient at large t,

$$\lim_{t\gg 0} K^{\dagger}(t) = K_0 = D\left(\frac{\pi}{x_{\mathrm{tr}}}\right)^2 = \frac{1}{2T}\left(\frac{\pi a}{x_{\mathrm{tr}}}\right)^2 = \frac{1}{2T}\left(\frac{\pi}{S}\right)^2. \tag{38}$$

This classical value for the Fickian reaction rate coefficient is represented in Fig. 3b as a horizontal line at later times.

7 Noise and Error Analysis of Statistical Simulation

When comparing the stochastic solution $K(t)$ to the analytical solution in the continuum limit $K^{\dagger}(t)$ in Fig. 3b and c, there are two principle sources of inaccuracy, both arising from the finite time difference approximation to the derivative $dP(t)/dt$ of the discontinuously valued stochastic survival probability $P(t)$. The first inaccuracy is the finite time difference error in approximating the true derivative. The second is statistical noise in counting the number of walkers annihilated within the time interval Δt over which the derivative is estimated. Whereas the first source of error is minimized by making the sampling time interval Δt as small as possible, the latter is minimized by making this time interval Δt as large as possible. By quantifying both sources of error, an optimal time difference interval can be determined for evaluating derivatives that will minimize error in the stochastic estimation of the reaction rate coefficient $K(t)$. The error analysis below will be particularly important for non-trivial wait-time distributions $\psi(\tau)$ whose probability distributions $P(t)$ and/or reaction rate coefficients $K(t)$ cannot be expressed analytically and must therefore be determined via stochastic simulation, only.

First, the finite-difference error in estimating the reaction coefficient will be quantified. The finite-difference derivative approximation to the reaction coefficient in

Eq. (23) will always *overestimate* the exact analytical solution by a small offset since the odd derivatives of a decay function are always negative [21], whereby $P'(t)$, $P'''(t) < 0$ in the Taylor expamsion:

$$\frac{P(t+\Delta t)-P(t-\Delta t)}{2\Delta t} = P'(t) + \Delta t^2 P'''(t)/6 + \dots \tag{39}$$

The overestimate $\epsilon_K^\dagger(t)$ in the reaction coefficient $K(t)$ can therefore be expressed as:

$$\epsilon_K^\dagger(t) = \frac{\Delta t^2}{6}\frac{|P'''(t)|}{P(t)} + \cdots . \tag{40}$$

For exponential-like decays with slowly varying decay coefficient $K(t)$ each successive derivative can be approximated as $P^{n+1}(t) \simeq -K(t)P^n(t)$ so that this relative offset can be approximated as

$$\frac{\epsilon_K^\dagger(t)}{K(t)} = \frac{\Delta t^2}{6}K^2(t) + \cdots \tag{41}$$

Thus, the systematic discrete derivative error will diverge as Δt^2 and would be minimized in the limit of small Δt.

On the other hand, the statistical noise $\delta K(t)$ in estimating $K(t)$ is minimized under larger sampling windows as Δt *increases*. The total noise fraction in the reaction coefficient $\delta K(t)/K(t)$ can be expressed as the quadrature sum of the noise fractions of the numerator and denominator in Eq. (12):

$$\left[\frac{\delta K(t)}{K(t)}\right]^2 = \left[\frac{\delta\frac{dP(t)}{dt}}{\frac{dP(t)}{dt}}\right]^2 + \left[\frac{\delta P(t)}{P(t)}\right]^2, \tag{42}$$

where the prefix δ represents the statistical noise for a given parameter. The noise in both terms in the right of Eq. (42) can be determined from the statistical fluctuation law $(\delta N)^2 = N$, where N corresponds to the relevant number of walkers for that term. To arrive at an expression for the first term, the relevant number is $N = \frac{1}{2\Delta t}|\frac{dP(t)}{dt}|W$, the average number of walkers that relax in the time interval $2\Delta t$ between points used in calculating the double-sided finite difference derivative in Eq. (23), and $\delta N = \delta\frac{dP(t)}{dt}W$ is the statistical fluctuation in the number of walkers within that time interval interval $2\Delta t$. Inserting both expressions into the fluctuation law gives:

$$\left[\delta\frac{dP(t)}{dt}W\right]^2 = \frac{1}{2\Delta t}|\frac{dP(t)}{dt}|\,W. \tag{43}$$

For the second term of Eq. (42), the fluctuation law again holds, where $N = P(t)W$ is the average number of walkers at time t, and $\delta N = \delta P(t)W$ is the statistical fluctuation in that number of walkers:

$$[\delta P(t)W]^2 = P(t)W. \tag{44}$$

Inserting both expressions back into Eq. (42) results in the following analytical prediction of noise in the stochastically simulated reaction coefficient,

$$\frac{\delta K^{\dagger}(t)}{K^{\dagger}(t)} = \sqrt{\frac{1}{P^{\dagger}(t)W}\left[\frac{1}{2K^{\dagger}(t)\Delta t}+1\right]} \approx \sqrt{\frac{1}{P^{\dagger}(t)2K^{\dagger}(t)W\Delta t}}. \tag{45}$$

For any useful relaxation study, the time interval $2\Delta t$ between discrete datapoints used for the numerical derivative should be much smaller than the characteristic decay time $1/K^{\dagger}(t)$, such that $2K^{\dagger}(t)\Delta t \ll 1$, hence the validity of the approximation to the right. Figure 3 plots this analytical estimation of the noise $\delta K^{\dagger}(t)$ from Eq. (45) (red dashed line), accurately predicting the standard deviation of the stochastic noise $\delta K(t)$ in the random walk simulation.

To find the value of Δt that minimizes the combined error from the noise $\delta K^{\dagger}(t)$ and offset $\epsilon_K^{\dagger}(t)$, the following expression needs to be minimized with respect to the choice of discrete time interval Δt for the finite difference derivative:

$$\frac{d}{d(\Delta t)}\left[\frac{\delta K^{\dagger}(t)}{K^{\dagger}(t)} + A\frac{\epsilon_K^{\dagger}(t)}{K^{\dagger}(t)}\right] = 0. \tag{46}$$

A multiplicative factor $A \gtrsim 1$ has been added to the offset term, so that the offset amplitude is buried well within the noise. Assuming a slowly varying reaction rate $K^{\dagger}(t)$ so that its derivatives can be neglected and picking a value of $A = 3$, the result becomes:

$$\Delta t(t) = \frac{1}{K^{\dagger}(t)}\left[\frac{1}{8P^{\dagger}(t)W}\right]^{\frac{1}{5}}. \tag{47}$$

Note that the stochastically derived $K(t)$ and $P(t)$ can also be inserted into Eq. (47) to determine the optimal discrete time interval Δt even though $K(t)$ itself depends on Δt via Eq. (23). In such a case, any value of Δt can be used for the discrete derivative in Eq. (23) to get a sufficiently accurate estimate of $K(t)$ for use in Eq. (47). Note, also, that the optimal time interval $\Delta t(t)$ for minimizing noise in the derivative is, itself, dependent on time. The 5th root of the bracketed term makes this dependence on the instantaneous survival probability $P^{\dagger}(t)$ very weak, so that a rough estimate of an average value within the time interval of interest is adequate. However, the reciprocal dependence on $K(t)$ is much stronger. Fortunately, in the present example of a Poissonian $\psi(\tau)$ wait time distribution, $K(t)$ rapidly approaches a constant value. But for time-dependent $K(t)$ such when $\psi(\tau)$ is governed, for example, by a power law [1–3], the time dependence of $K(t)$ must be considered.

It is therefore recommended that the smallest value of Δt be chosen within the data range of interest,

$$\Delta t_0 = \min\{\Delta t(t)\}. \tag{48}$$

Under the condition of minimal Δt_0, any error is dominated by noise $\delta K(t)$ around the correct mean value, rendering the systematic offset $\epsilon_K^\dagger(t)$ negligible by comparison. For example, if $K(t)$ is approximately constant, this means the smallest value Δt_0 will occur at the *beginning* of the time interval of interest where $P(t)$ is largest. Conversely, if $K(t)$ decreases with time faster than the 5th root of $P(t)$, then this means the smallest value Δt_0 will occur at the *end* of the time interval of interest. Once one knows whether the beginning or the end of the time interval t in Eq. (48) should be considered for Δt_0, Eqs. (45) and (47) can be combined and inverted to determine the number of walkers W required to achieve the appropriate minimum error tolerance $\delta K(t)/K(t)$:

$$W = \frac{1}{\sqrt{2}\,P(t)} \left(\frac{1}{\delta K/K(t)} \right)^{\frac{5}{2}}. \tag{49}$$

8 Results

The results below show quantitative agreement between the stochastic simulation of the random walk with a discrete number of steps and the analytical result from the spatial continuum limit, while importantly also accurately predicting the margin of error for the stochastic result. In the general scenario for a given wait-time distribution $\psi(t)$, an initial stochastic simulation with arbitrary Δt and arbitrary W would be run to get an estimate of the $P(t)$ and $K(t)$ values for a given time range of interest. Then these values along with the desired noise tolerance $\delta K/K$ would be used to estimate both the necessary number of walkers W per Eq. (49) and the corresponding optimal Δt_0 value per Eqs. (47) and (48). If a particularly broad time range has $P(t)$ and $K(t)$ values that vary by more than an order of magnitude, the time range can be broken into temporal subsegments, each with a different W and Δt_0 value for error minimization.

In the present case, $P^\dagger(t)$ and $K^\dagger(t)$ can be taken from the asymptotic exponential decay form in the analytical solution. Equation (38) yields the following analytical value for the asymptotic rate coefficient,

$$\lim_{t\to\infty} K^\dagger(t) = K_0 = \pi^2/4 \simeq 2.4674, \tag{50}$$

and if we assume the desired time range of interest is around $K_0 t = 1.5$, then $P^\dagger(t) \simeq 0.28$ from Eq. (37). If the desired accuracy is $\delta K/K = 0.2\%$, then the number of walkers necessary to run a stochastic simulation from Eq. (49) is circa $W \simeq 10^7$, and the optimal step time interval for the lowest noise stochastic simulation from Eq. (47) is $\Delta t_0 \simeq 0.014$. In anticipation of this result, these are exactly the parameters used in the data shown in Fig. 3.

The numerical accuracy of the stochastic simulation can now be quantified. The mean statistical value $\langle K(t)\rangle$ and the standard deviation $\delta K(t)$ for data between $1 < K_0 t < 2$ are calculated to be:

$$\langle K(t)\rangle \pm \delta K(t) = 2.465 \pm 0.0056. \tag{51}$$

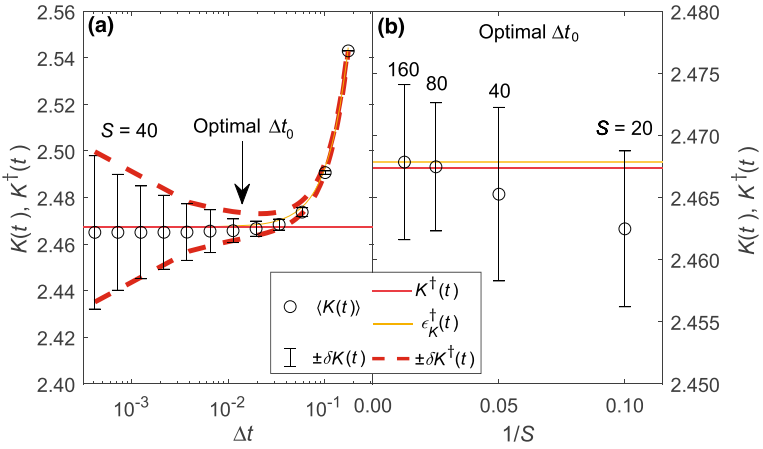

Fig. 5 Analysis of statistical error in the stochastic simulation of a diffusion-limited unimolecular reaction. **a** The average reaction rate coefficient $\langle K(t)\rangle$ (open circles) and standard deviation $\pm\delta K(t)$ (error bars) of the stochastic dataset sampled from $1 < K_0 t < 2$ are evaluated for different step time intervals Δt. The optimal Δt_0 from Eq. (47) indicated with a vertical arrow clearly shows a minimum in the total error due to the combination of statistical noise (dominating left of Δt_0) and discrete derivative offset (dominating right of Δt_0). This mean value and error compare favorably to analytical value $K^\dagger(t)$ (red solid line) and predicted error $\epsilon^\dagger(t) \pm \delta K^\dagger(t)$, respectively, from the analytical expression in Eqs. (41) and (45), respectively. The parameters in (**a**) are identical to those in Fig. 3. The residual discrepancy in panel (a) to the left of Δt_0 between the average statistical value $\langle K(t)\rangle$ and the analytical result $K^\dagger(t)$ of circa 0.007 is an artifact of the discrete versus continuum cases, respectively. **b** A zoomed in comparison of the standard deviations under optimal Δt_0 with varying step number S shows eventual convergence of the statistical average $\langle K(t)\rangle$ to the analytical continuum value $K^\dagger(t) + \epsilon^\dagger(t)$ as $S \to \infty$ or $1/S \to 0$.

The mean value is within 0.1% of the analytical result of Eq. (50), and the standard deviation is 0.23%, which matches the desired error margin, validating the statistical method proposed here.

To further demonstrate that Δt_0 per Eq. (47) is, in fact, the optimal step time for minimal noise, a range of step times Δt was tested in Fig. 5a. Statistical ensembles of $K(t_r)$ generated from different values of Δt are analyzed between times $t = 1/K_0$ and $2/K_0$, and the results are compared to the predicted accuracy from the above analysis. Once again, the ensemble averages $\langle K(t)\rangle$ are plotted with open circles and the statistical standard deviations $\pm\delta K(t)$ with error bars. For comparison, the analytically predicted asymptotic reaction rate coefficient K_0 is plotted with a horizontal red line. with predicted offset error $\epsilon_K^\dagger(t)$ from Eq. (41) plotted with a yellow line, and the predicted noise error $\delta K^\dagger(t)$ with a dashed red line. As predicted from Eq. (45), the noise $\pm\delta K(t)$ in Fig. 5a diverges to the left as $\Delta t \to 0$ like $\pm\Delta t^{-1/2}$, and the offset error $\epsilon_K^\dagger(t)$ (yellow line) diverges to the right as $\Delta t \to \infty$ like $+\Delta t^2$. In the middle, Eq. (47) proposes the optimal finite difference time interval Δt_0 to minimize error with a vertical arrow at $\Delta t_0 = 0.014$. Overall, Fig. 5a shows excellent quantitative agreement between the values from the statistical ensemble and the predicted analytical value and accuracy:

$$\langle K(t)\rangle \pm \delta K(t) \simeq K^\dagger(t) + \epsilon_K^\dagger(t) \pm \delta K^\dagger(t). \tag{52}$$

$$
\begin{aligned}
K(t_r) &: \text{stochastic} \\
\langle K(t)\rangle &: \text{stochastic average} \\
\pm\delta K(t) &: \text{standard deviation}
\end{aligned}
$$

$$
\begin{aligned}
K^{\dagger}(t) &: \text{analytical} \\
\epsilon_K^{\dagger}(t) &: \text{predicted offset error} \\
\pm\delta K^{\dagger}(t) &: \text{predicted noise error}
\end{aligned}
$$

The minor discrepancy to the left of Fig. 5a between the statistical average $\langle K(t)\rangle$ and the analytical continuum value $K^{\dagger}(t)$ can be shown to be an artifact of the discrete step number. In Fig. 5b the statistical mean and standard deviation are plotted versus the reciprocal step count $1/S$ at various step count values S for the optimal Δt_0 derivative time interval. As the step count S is increased to the left, the asymptotic value $\langle K(t)\rangle$ in the limit of $S \to \infty$ approaches the continuum prediction of $K^{\dagger}(t) + \epsilon^{\dagger}(t)$. Note that by design, the systematic offset error of $\epsilon^{\dagger}(t)$ is much less than the standard deviation $\delta K^{\dagger}(t)$.

9 Conclusion

This work has shown how to stochastically simulate a continuous time random walk model of a diffusion-limited unimolecular reaction with arbitrary wait-time distribution function $\psi(t)$. The characteristic model parameters can be reliably quantified within a prespecified error tolerance and can be reduced arbitrarily by increasing the number of walkers. The accuracy of this approach is confirmed using a simple Poissonian wait-time distribution and simple binary left-right step distribution that yields the standard diffusion limit at long times. Initial transient behavior also reveal the relaxation times of the higher spatial harmonics in the starting spatial distribution of walkers between reactive trap sites. These stochastic simulations have the potential to be more powerful than analytical solutions when modeling experimental systems whose wait-time distributions $\psi(\tau)$ defy an analytical CTRW solution. The stochastic model presented in this work can easily be extended to higher dimensions, as well as to bimolecular and anomalous diffusion-limited reactions.

Acknowledgements This work was supported in part by NSF Grants DMREF-1729016, DMR-1720139, and ECCS-1912694, with additional support provided by Leslie and Mac McQuown.

Declarations

Conflict of interest The authors declare that there are no conflicts of interest that are directly or indirectly related to the work submitted for publication. All data in the manuscript is freely available from the authors upon request.

Appendix: Continuum Limit for Survival Probability Distribution

The continuum expressions for the diffusion-limited reaction are detailed below. Using the following definition of the Fourier transform,

$$\widetilde{p}(k,t) = \frac{1}{\sqrt{2\pi}} \int p(x,t) e^{-ikx} dx \tag{53}$$

Eq. (33) can be expressed as

$$\widetilde{p}(k,t) = \sum_{j=-\infty}^{\infty} (-1)^j \left[\frac{1}{\sqrt{2\pi}} \int G\left(x - j x_{\mathrm{tr}}, t\right) e^{-ikx} dx \right] \tag{54}$$

Taking advantage of the translation property of Fourier transforms, this can be written as

$$\begin{aligned} \widetilde{p}(k,t) &= \sum_{j=-\infty}^{\infty} (-1)^j e^{-ij x_{\mathrm{tr}} k} \widetilde{G}\left(k,t\right) \\ &= \widetilde{G}\left(k,t\right) \left[\sum_{j=-\infty}^{\infty} e^{i2j x_{\mathrm{tr}} k} - \sum_{j=-\infty}^{\infty} e^{i(2j-1) x_{\mathrm{tr}} k} \right] \\ &= \widetilde{G}\left(k,t\right) \left(1 - e^{-i x_{\mathrm{tr}} k}\right) \sum_{j=-\infty}^{\infty} e^{i2j x_{\mathrm{tr}} k} . \end{aligned} \tag{55}$$

where the Fourier transform of $G(x,t)$ is:

$$\begin{aligned} \widetilde{G}(k,t) &= \frac{1}{\sqrt{2\pi}} \int_{-\infty}^{\infty} (4\pi Dt)^{-\frac{1}{2}} \exp\left(-\frac{x^2}{4Dt}\right) e^{-ikx} dx \\ &= \frac{1}{\sqrt{2\pi}} e^{-k^2 Dt} . \end{aligned} \tag{56}$$

Applying the Poisson summation formula, yields

$$\sum_{j=-\infty}^{\infty} e^{i2j x_{\mathrm{tr}} k} = \frac{\pi}{x_{\mathrm{tr}}} \sum_{\nu=-\infty}^{\infty} \delta\left(k - \frac{\pi \nu}{x_{\mathrm{tr}}}\right) . \tag{57}$$

Inverting the Fourier transform and using Eqs. (55) and (57), the final expression for the time-dependent probability distribution becomes,

$$p^{\dagger}(x,t) = \frac{1}{\sqrt{2\pi}} \int \frac{1}{\sqrt{2\pi}} e^{-k^2 Dt} e^{ikx} \left(1 - e^{-ix_{\mathrm{tr}}k}\right) \times \frac{\pi}{x_{\mathrm{tr}}} \sum_{\nu=-\infty}^{\infty} \delta\left(k - \frac{\pi\nu}{x_{\mathrm{tr}}}\right) dk \tag{58}$$

$$= \frac{1}{2x_{\mathrm{tr}}} \sum_{\nu=-\infty}^{\infty} \exp\left[-\nu^2 \left(\frac{\pi}{x_{\mathrm{tr}}}\right)^2 Dt\right] \times \exp\left[i\nu\left(\frac{\pi}{x_{\mathrm{tr}}}\right)x\right] \left[1 - \exp\left(-i\nu\pi\right)\right] \tag{59}$$

$$= \frac{1}{x_{\mathrm{tr}}} \sum_{\nu \text{ odd}} \exp\left[-\nu^2 \left(\frac{\pi}{x_{\mathrm{tr}}}\right)^2 Dt\right] \times \exp\left[i\nu\left(\frac{\pi}{x_{\mathrm{tr}}}\right)x\right] \tag{60}$$

$$= \frac{2}{x_{\mathrm{tr}}} \sum_{\nu=0}^{\infty} \exp\left\{-\left[\frac{\pi(2\nu+1)}{x_{\mathrm{tr}}}\right]^2 Dt\right\} \times \cos\left\{\left[\frac{\pi(2\nu+1)}{x_{\mathrm{tr}}}\right]x\right\}. \tag{61}$$

Spatial integration will then determine the survival probability as a function of time,

$$P^{\dagger}(t) = \int_{-x_{\mathrm{tr}}/2}^{x_{\mathrm{tr}}/2} p^{\dagger}(x,t)dx \tag{62}$$

$$= \frac{2}{x_{\mathrm{tr}}} \sum_{\nu=0}^{\infty} \exp\left\{-\left[\frac{\pi(2\nu+1)}{x_{\mathrm{tr}}}\right]^2 Dt\right\} \times \int_{-x_{\mathrm{tr}}/2}^{x_{\mathrm{tr}}/2} \cos\left\{\left[\frac{\pi(2\nu+1)}{x_{\mathrm{tr}}}\right]x\right\}dx \tag{63}$$

$$= \frac{2}{x_{\mathrm{tr}}} \sum_{\nu=0}^{\infty} \exp\left\{-\left[\frac{\pi(2\nu+1)}{x_{\mathrm{tr}}}\right]^2 Dt\right\} \times \left[\frac{2x_{\mathrm{tr}}}{\pi(2\nu+1)}(-1)^{\nu}\right] \tag{64}$$

$$= \frac{4}{\pi} \sum_{\nu=0}^{\infty} \frac{(-1)^{\nu}}{2\nu+1} \exp\left\{-\left[\frac{\pi(2\nu+1)}{x_{\mathrm{tr}}}\right]^2 Dt\right\}. \tag{65}$$

References

1. Shlesinger MF (2017) Origins and applications of the Montroll–Weiss continuous time random walk. Eur Phys J B 90:93. https://doi.org/10.1140/epjb/e2017-80008-9
2. Scher H, Montroll EW (1975) Anomalous transit-time dispersion in amorphous solids. Phys Rev B 12:2455. https://doi.org/10.1103/PhysRevB.12.2455

3. Shlesinger MF, Montroll EW (1984) On the Williams–Watts function of dielectric relaxation. PNAS 81:1280–1283. https://doi.org/10.1073/pnas.81.4.1280
4. Ngai KL, Liu F-S (1981) Dispersive diffusion transport and noise, time-dependent diffusion coefficient, generalized Einstein–Nernst relation, and dispersive diffusion-controlled unimolecular and bimolecular reactions. APS Phys 24:1049. https://doi.org/10.1103/PhysRevB.24.1049
5. Shlesinger MF (2017) Origins and applications of the Montroll–Weiss continuous time random walk. Eur Phys J B 90:93. https://doi.org/10.1140/epjb/e2017-80008-9
6. Shlesinger MF (1979) Electron scavenging in glasses. J Chem Phys 70:4813. https://doi.org/10.1063/1.437370
7. Kenkre VM, Montroll EW, Shlesinger MF (1973) Generalized master equations for continuous-time random walks. J Stat Phys 9:45–50. https://doi.org/10.1007/BF01016796
8. Montroll EW, Scher H (1973) Random walks on lattices. IV. continuous-time walks and influence of absorbing boundaries. J Stat Phys 9:101–135. https://doi.org/10.1007/BF01016843
9. Montroll EW, Weiss GH (1965) Random walks on lattices II. J Math Phys 6:167. https://doi.org/10.1063/1.1704269
10. Laidler KJ, Meiser JH (1982) Physical chemistry. Benjamin/Cummings, Menlo Park, CA
11. Karaman MM, Sui Y, Wang H, Magin RL, Li Y, Zhou XJ (2016) Differentiating low- and high-grade pediatric brain tumors using a continuous-time random-walk diffusion model at high b-values. Mag Reson Med 76:1149. https://doi.org/10.1002/mrm.26012
12. Berezhkovskii A, Weiss GH (2008) Propagators and related descriptors for non-Markovian asymmetric random walks with and without boundaries. J Chem Phys 128:044914. https://doi.org/10.1063/1.2830254
13. Metzler R, Klafter J (2000) The random Walk's guide to anomalous diffusion: a fractional dynamics approach. Phys Rep 339:1–77
14. Montroll EW (1964) Random walks on lattices. Am Math Soc 16:193–220. https://doi.org/10.1090/psapm/0161378
15. Klafter J, Sokolov IM (2011) First steps in random walks. Oxford University Press, New York
16. Montroll EW, Shlesinger MF (1984) On the wonderful world of random walks. In: Lebowitz JL, Montroll EW (eds) Studies in statistical mechanics, vol 11. Elsevier Science Pub. Co., New York, pp 46–116
17. Scher H, Lax M (1973) Stochastic transport in a disordered solid. I. Theory. Phys Rev B 7:4491. https://doi.org/10.1103/PhysRevB.7.4491
18. Montroll EW (1969) Random walks on lattices III. Calculation of first? Passage times with application to exciton trapping on photosynthetic units. J Math Phys 10:753. https://doi.org/10.1063/1.1664902
19. Hemenger RP, Pearlstein RM, Lakatos-Lindenberg K (1972) Incoherent exciton quenching on lattices. J Math Phys 13:1056. https://doi.org/10.1063/1.1666085
20. Gentle JE (2003) Random number generation and Monte Carlo methods. Springer, New York. https://doi.org/10.1007/b97336
21. Zorn R (2002) Logarithmic moments of relaxation time distributions. J Chem Phys 116:3204. https://doi.org/10.1063/1.1446035

Publisher's Note Springer Nature remains neutral with regard to jurisdictional claims in published maps and institutional affiliations.

Springer Nature or its licensor (e.g. a society or other partner) holds exclusive rights to this article under a publishing agreement with the author(s) or other rightsholder(s); author self-archiving of the accepted manuscript version of this article is solely governed by the terms of such publishing agreement and applicable law.